Supplementary Material

Single-cell ionic current phenotyping explains stem cell-derived cardiomyocyte action potential morphology

Alexander P. Clark[1], Siyu Wei[2], Kristin Fullerton[3],
Trine Krogh-Madsen,[3,4] David J. Christini[1,2]

---

1 Methods

1.1 iPSC-CM cell culture and electrophysiological setup

The *in vitro* data was previously published [1].

Frozen iPSC-CMs were thawed from five different vials that were purchased from the Stanford Cardiovascular Institute Biobank. Prior to patch-clamp recording, each cell was plated on a coverslip and had been independently cultured for 3-13 days in a 24-well plate. These cells were derived from an African-American female donor in a process approved by Stanford University Human Subjects Research Institutional Review Board.

Cells were prepared for electrophysiological experiments following the steps described in [1]. Briefly, cells were thawed and cultured as a monolayer in one well of a 6-well plate precoated with 1% Matrigel. Cells were cultured with RPMI media (Fisher/Corning 10-040-CM) containing 5% FBS and 2% B27 and kept in an incubator at 37 °C, 5% CO_2, and 85% humidity. After 48 hours, cells were lifted with 1 mL Accutase, diluted to 100,000 cells/mL, and replated on 124 sterile 8 mm coverslips precoated with 1% Matrigel. Cells were cultured with RPMI media that was swapped every 48 hours. Cells were patched between days 5 and 15 after thaw.

Voltage clamp and current clamp recordings were acquired from 40 cells using the perforated patch technique and an amplifier equipped with a voltage follower circuit (Model 2400; A-M Systems, Sequim, WA). We excluded one cell from the analyses in this study because it had spontaneous alternans with inconsistent AP features. All cells had a pre-rupture seal of >300 MΩ.

1.2 Voltage clamp protocol

We have previously developed a voltage clamp protocol consisting of multiple short segments, each designed to isolate one key ionic current [1]. The protocol was designed using optimization techniques and a mathematical model of iPSC-CMs [2] to maximize, one at a time, the contribution to total current by each of seven key currents: I_{Kr}, I_{CaL}, sodium current (I_{Na}), transient outward K^+ current (I_{to}), inward rectifier K^+ current (I_{K1}), funny current (I_f), and slow delayed rectifier K^+ current (I_{Ks}).

During our analysis, we found that the current measured 100 ms after a depolarizing step to 6 mV (I_{6mV}) was substantially different in many cells from that predicted by the mathematical model and we therefore included I_{6mV} as an 8th current measure.

For each current-isolating segment, we quantified the recorded total current I_{out} using either the minimum or the average over a 2 ms span centered at the following values: I_{6mV} (600 ms, average), I_{Kr} (1262 ms, average), I_{CaL} (1986 ms, minimum), I_{Na} (2760 ms, minimum), I_{to} (3641 ms, average), I_{K1} (4300 ms, average), I_f (5840 ms, average), and I_{Ks} (9040 ms, average).

1.3 AP feature calculations

The transmembrane potential of each cell was recorded for 10 s. Of the 39 cells, 12 were not spontaneously beating. We computed a minimal potential (MP) for these non-spontaneous cells.

For cells that were spontaneously beating, we computed their MP (in this case, the minimum voltage during the AP), action potential duration at 90% repolarization (APD_{90}), cycle length (CL), and maximal upstroke velocity (dV/dt_{max}). The average of each feature was calculated for all cells that produced more than one AP during the 10 s recording.

1.4 iPSC-CM mathematical models

For comparison and to guide the analysis of our experimental data, we used two different mathematical models of iPSC-CM electrophysiology: the Paci et al. model [3] and the Kernik et al. model [2]. We set the cell capacitance (C_m) of these models to 45 pF, which is centrally located in the range (18-98 pF) of the capacitances for cells used in this study.

To avoid long transients and to better simulate our perforated patch experimental setup, we fixed intracellular sodium and potassium concentrations ($[Na^+]_i$ and $[K^+]_i$) to their baseline steady state values (taken after 1000 s of spontaneous or paced current clamp simulation).

Because the leak through the imperfect pipette-membrane seal during single-cell patch-clamp experiments can substantially impact the electrophysiological recordings in these cells, we included a linear leak current (I_{leak}) in the mathematical models [4]. We used a baseline value of 2 GΩ for the seal resistance.

In addition to the seal-leak current, for voltage clamp simulations, we included explicit modeling of the following

experimental artifacts: liquid junction potential offset (-2.8 mV), access resistance (20 MΩ), and series resistance (R_s) compensation (70%), including supercharging [5, 6].

1.5 Population of models and sensitivity analysis

A population of 500 individuals with unique parameters sets was generated using both the Paci and Kernik models with experimental artifact equations by randomly sampling conductances of I_{Na}, I_{CaL}, I_{Kr}, I_{Ks}, I_{to}, I_{K1}, I_f, I_{leak}, sodium calcium exchange current (I_{NaCa}), sodium potassium pump current (I_{NaK}), sodium background current (I_{bNa}), calcium background current (I_{bCa}), as well as C_m and R_s from a log uniform distribution between 0.25 and 4x their baseline values. Of the 500 Paci models, 18 were excluded due to numerical integration issues. The Kernik and Paci populations produced 150 and 194 spontaneously beating individuals, respectively. All individuals (whether spontaneously beating or not) were used to calculate the MP. Only spontaneously beating individuals were used to calculate dV/dt_{max}, APD_{90}, and CL.

We used a Spearman correlation to determine the sensitivity of the current-isolating time points to these parameters.

1.6 Linear regression

A linear least-squares regression was used to compare ionic currents and AP features for both the *in vitro* and the *in silico* data. A Spearman correlation coefficient and p-value were calculated for these data.

1.7 Software and simulations

Simulations were performed in Myokit v1.33.7 [7]. Additional analysis was done in Python using NumPy v1.21.6 and SciPy v1.7.3 [8].

All data, code and models can be accessed from GitHub (`https://github.com/Christini-Lab/ap-vc-correlations.git`).

2 Supplementary figures

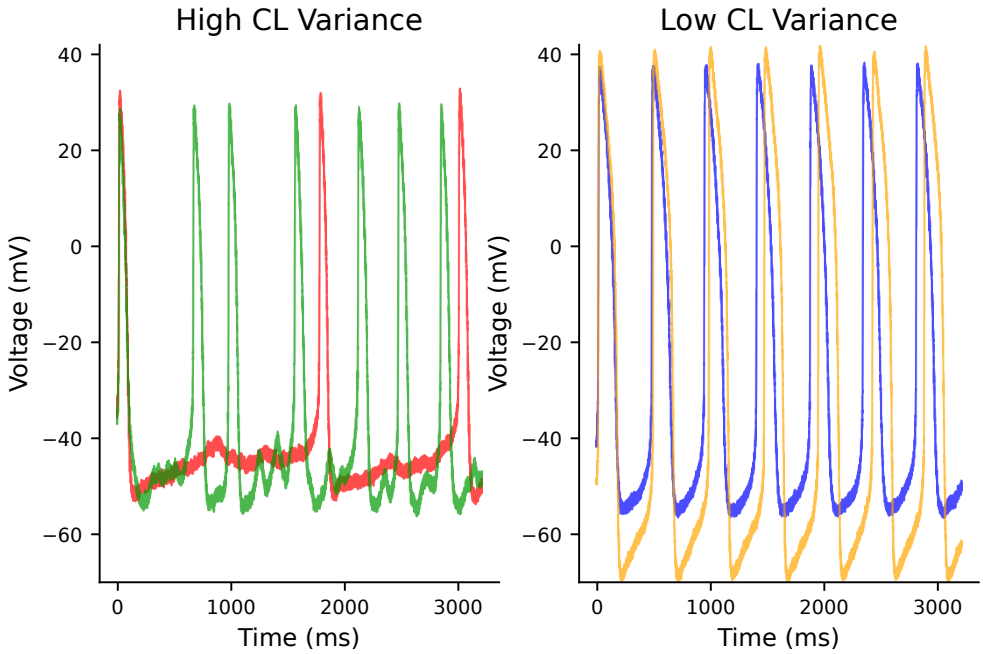

Figure 1: **Cells with high (left) and low (right) variance in cycle length**. High-variance cells have an irregular diastolic depolarization ramp and varying takeoff potential, while low-variance cells show consistent, very regular AP morphologies.

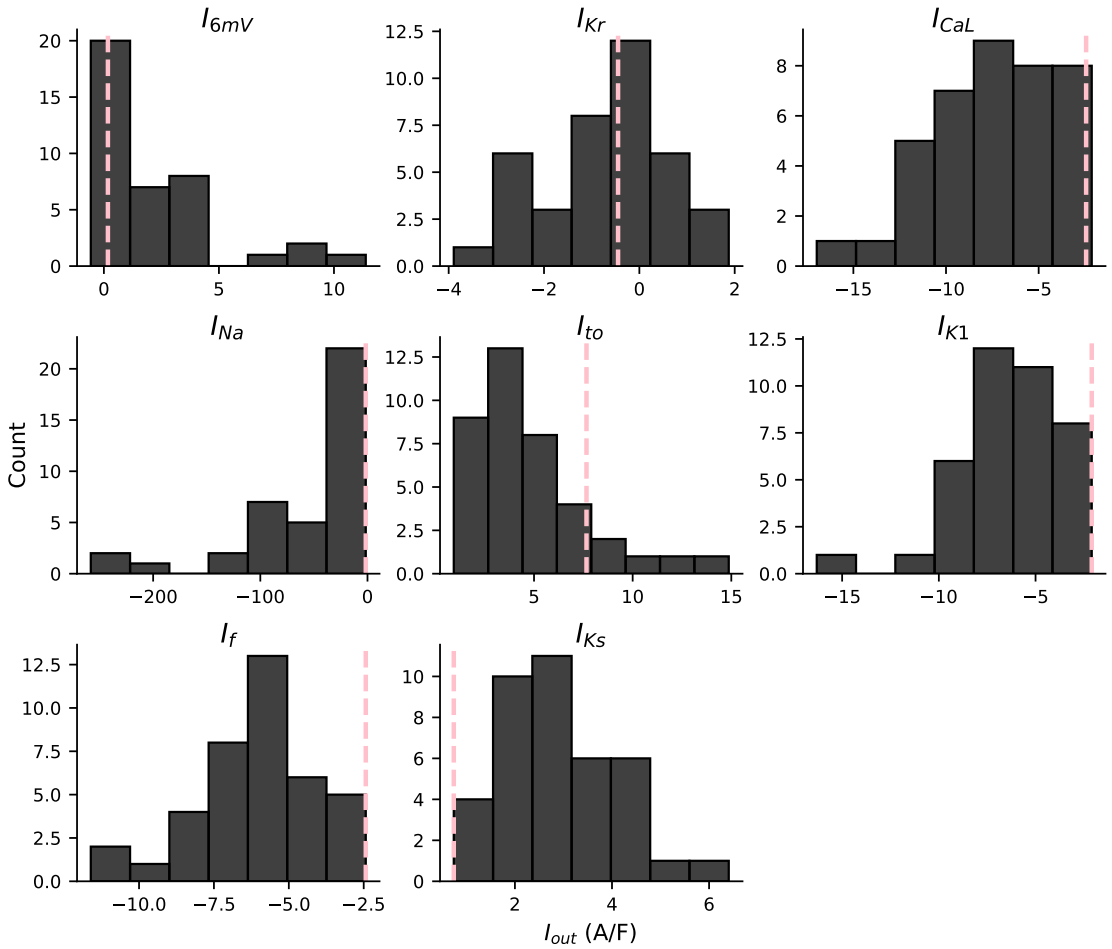

Figure 2: **I_{out} distribution at the eight current-isolating time points.** Histograms display the distribution of recorded current values at each of the eight time points. The pink dashed line shows I_{out} values for the outlier cell.

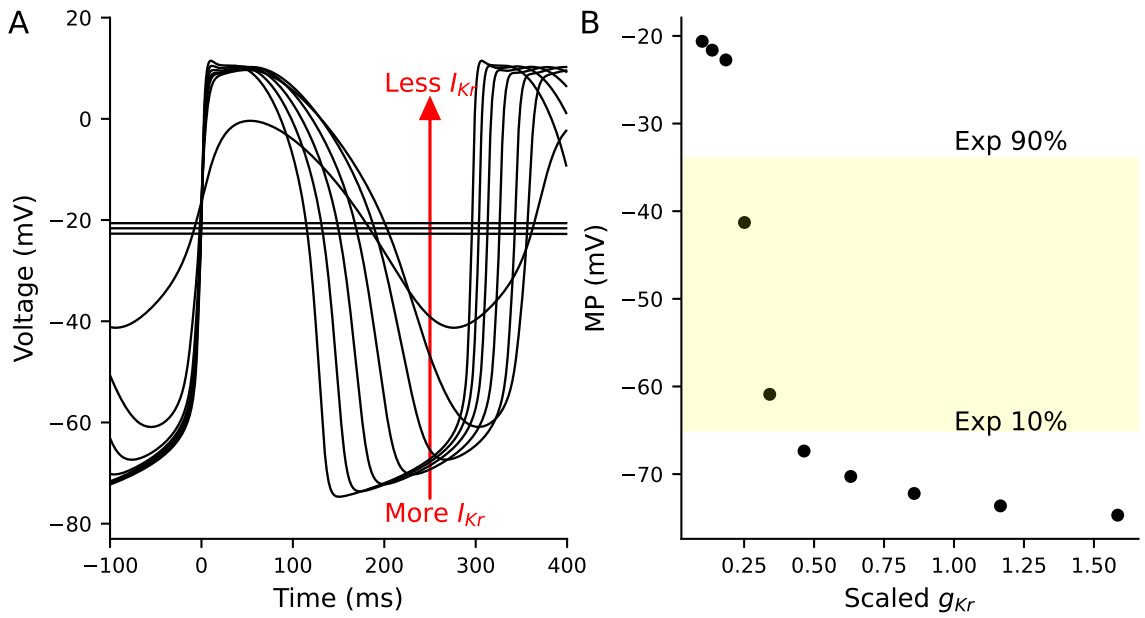

Figure 3: **AP simulations of a Kernik-Clancy model with a 2 GΩ seal resistance and varying levels of g_{Kr} A**, APs generated by running the model with varying levels of g_{Kr} from 0.1 to 1.6 times the baseline Kernik-Clancy value (0.218025 nS/pF). The arrow indicates that depolarized cells have less I_{Kr} (i.e., smaller g_{Kr}). **B**, Relationship between g_{Kr} and MP for cells plotted in **A**. The yellow highlighted region represents the 10% to 90% range of MP values from cells in this study.

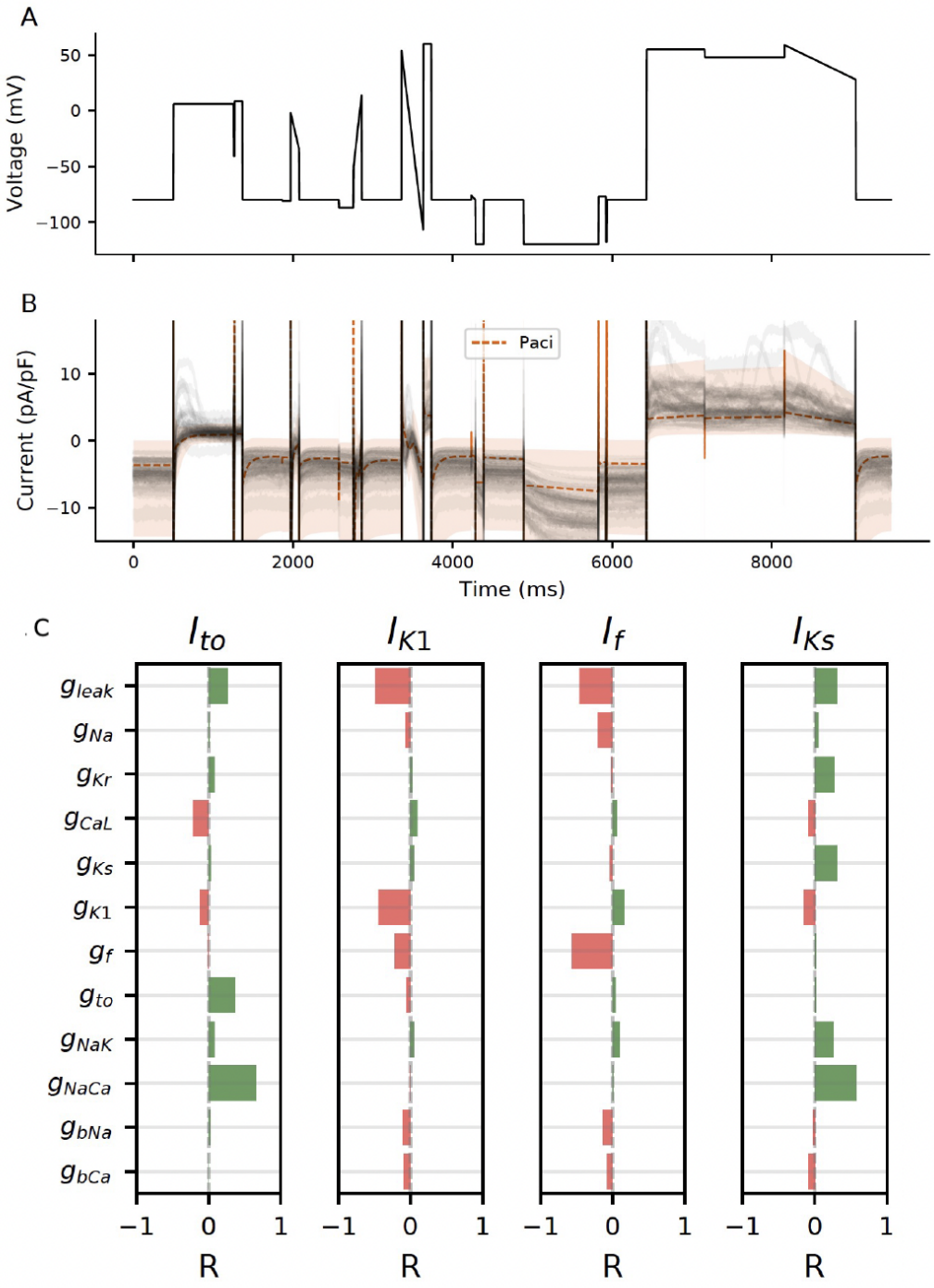

Figure 4: **A population of Paci models compared to experimental data.** 500 Paci individuals were generated by varying ionic current conductances and experimental artifact parameters (see Methods). The dashed orange line shows the average I_{out} for all models, and the shaded region is the range of values for all models. The experimental data are displayed in gray. **C**, Correlations calculated between model parameter values (primarily conductances; e.g., g_{Kr}) and I_{out} during each of these four segments. Each current is sensitive to its own conductance, with outward currents (I_{to} and I_{Ks}) having a positive correlation and inward currents (I_{K1} and I_f) showing as a negative correlation to their own conductance. Each current is also sensitive to g_{leak}. Both I_{to} and I_{Ks} have a surprisingly strong sensitivity to g_{NaCa}.

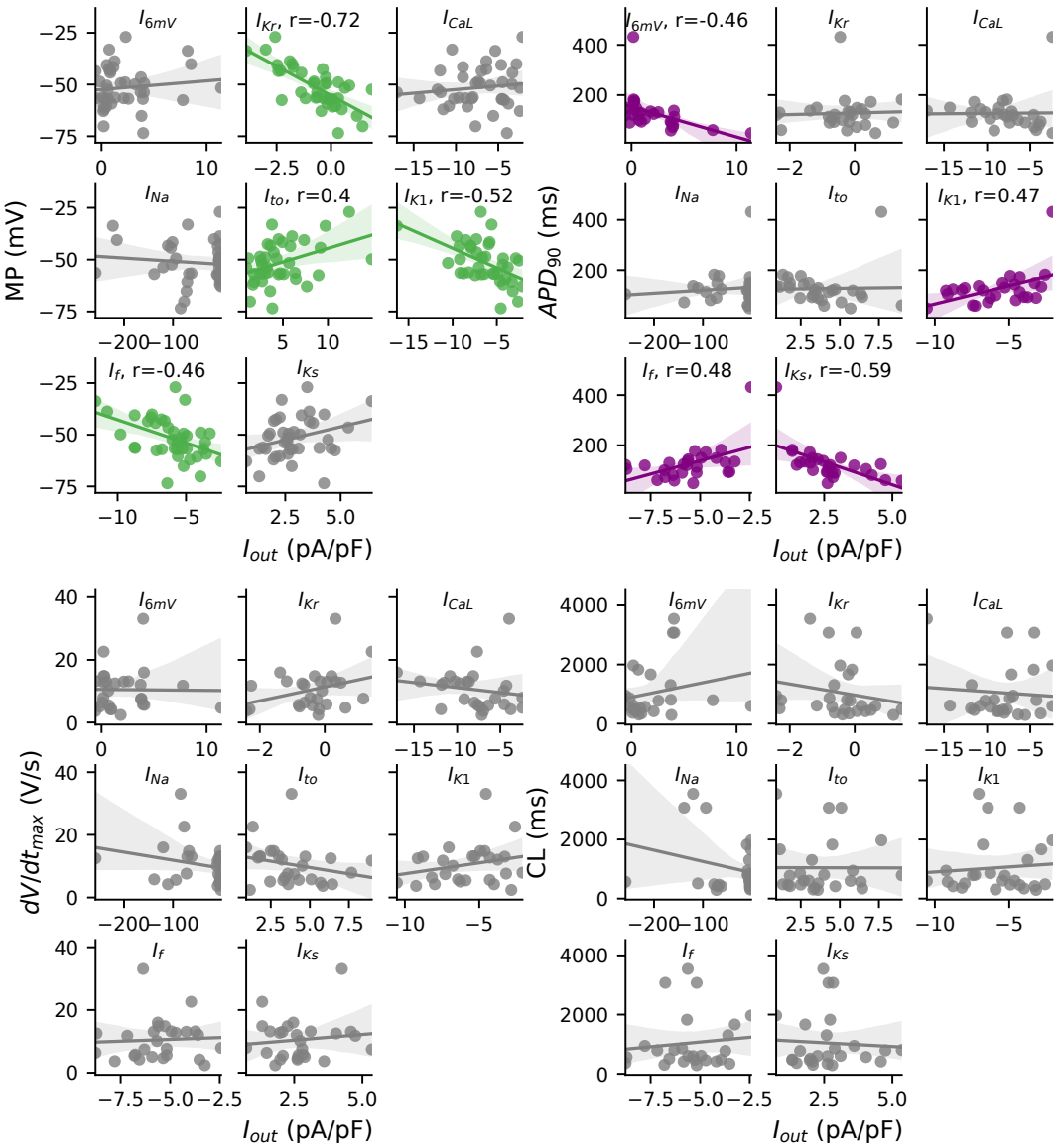

Figure 5: **AP parameter and current correlations for *in vitro* cells**. Correlations between AP metrics and current-isolating segments. Non-gray colors indicate correlations that met threshold for statistical significance.

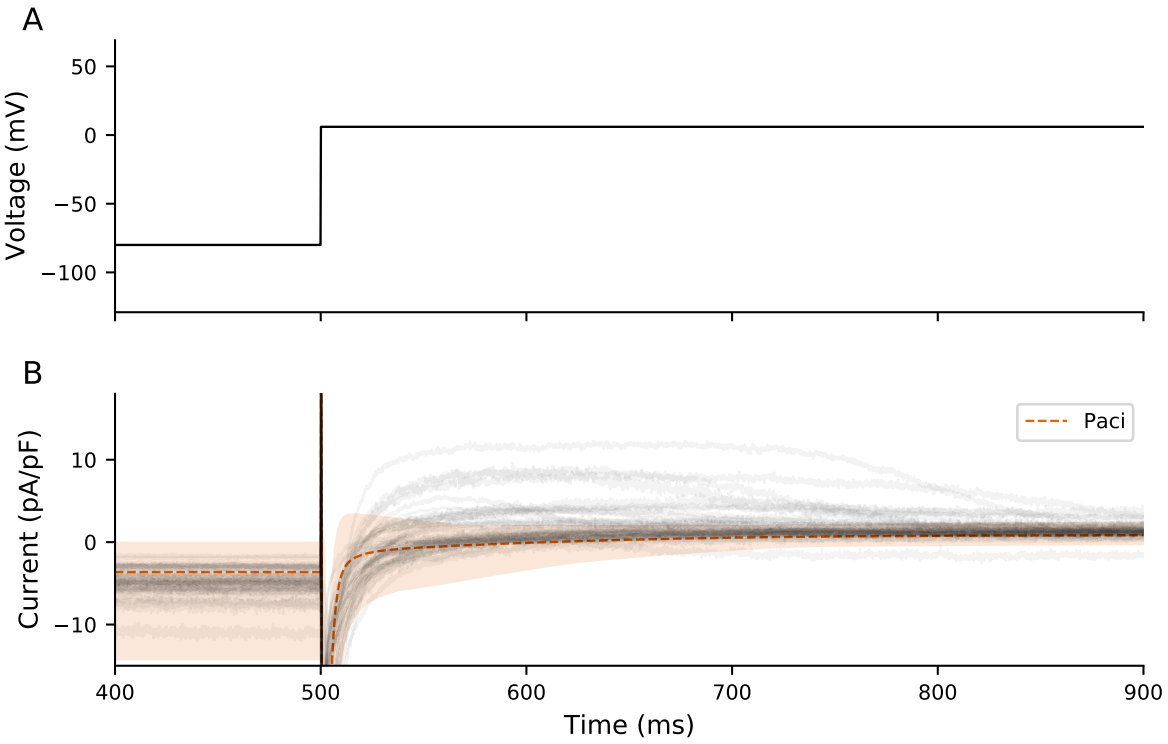

Figure 6: **Comparison of Paci and experimental I_{6mV}.** Experimental (gray) and range of Paci model traces (shaded orange) during I_{6mV} voltage step. The experimental responses for many of the cells (11/39) during this segment are more positive than any individual in the model population.

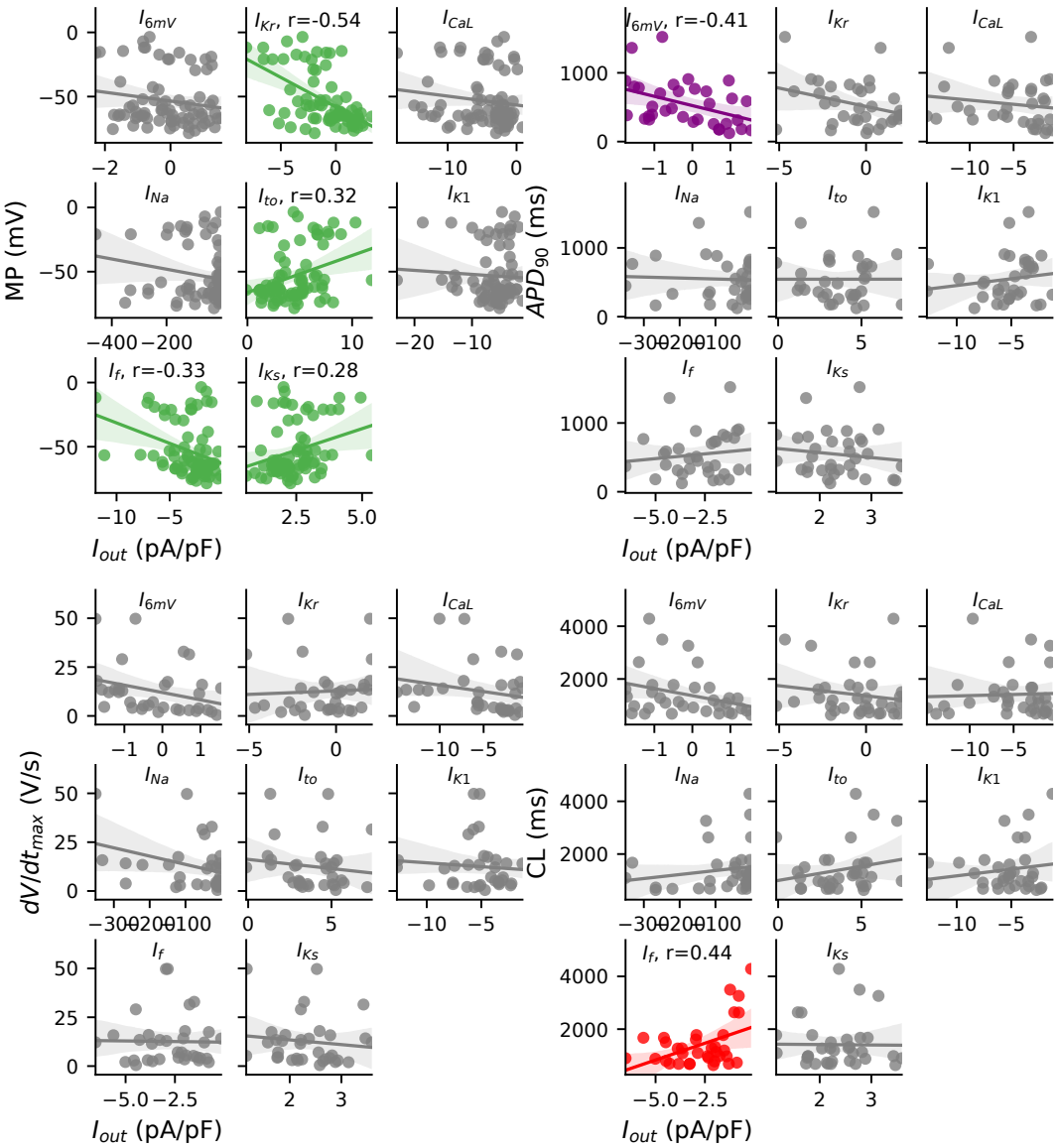

Figure 7: **AP parameter and current correlations for Paci-based model population**. Correlations between AP metrics and current-isolating segments. Non-gray colors indicate correlations that met threshold for statistical significance. There are no statistically significant correlations between dV/dt_{max} and any of the current-isolating segments. I_{Kr} is the main determinant of MDP, I_f the main determinant of CL, and I_{6mV} the main determinant of APD_{90}.

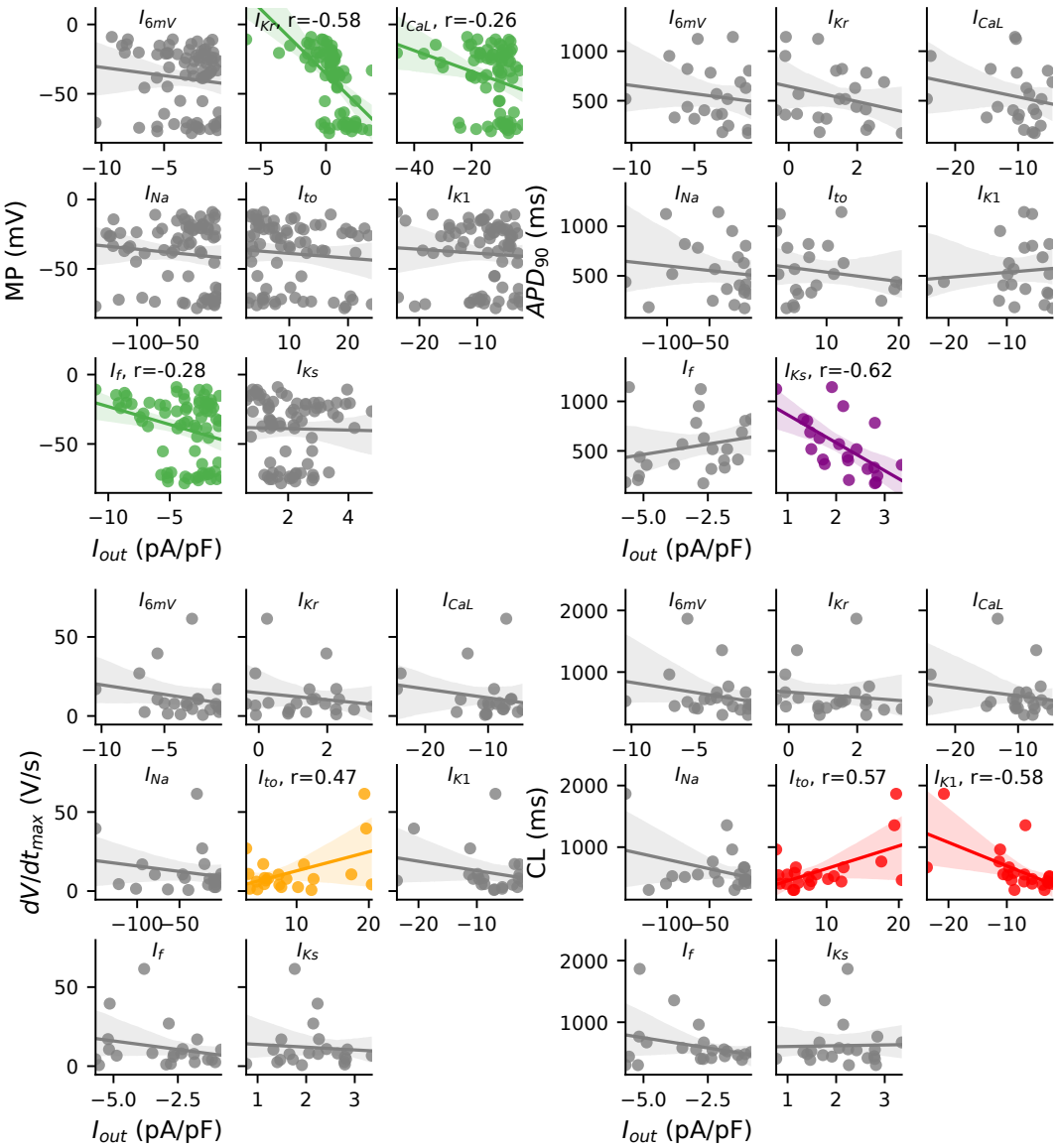

Figure 8: **AP parameter and current correlations for Kernik-based model population**. Correlations between AP metrics and current-isolating segments. Non-gray colors indicate correlations that met threshold for statistical significance. I_{to} correlate with dV/dt_{max}, I_{Ks} with APD_{90}, and both I_{to} and I_{K1} with CL. I_{Kr} is the main determinant of MDP.

References

1. Clark, A. P., Wei, S., Kalola, D., Krogh-Madsen, T. & Christini, D. J. An in silico-in vitro pipeline for drug cardiotoxicity screening identifies ionic pro-arrhythmia mechanisms. *British journal of pharmacology* **179,** 4829–4843. ISSN: 1476-5381. http://www.ncbi.nlm.nih.gov/pubmed/35781252%20http://www.pubmedcentral.nih.gov/articlerender.fcgi?artid=PMC9489646 (Oct. 2022).
2. Kernik, D. C. *et al.* A computational model of induced pluripotent stem-cell derived cardiomyocytes incorporating experimental variability from multiple data sources. *Journal of Physiology* **597,** 4533–4564. ISSN: 14697793 (2019).
3. Paci, M., Hyttinen, J., Aalto-Setälä, K. & Severi, S. Computational Models of Ventricular- and Atrial-Like Human Induced Pluripotent Stem Cell Derived Cardiomyocytes. *Annals of Biomedical Engineering* **41,** 2334–2348. ISSN: 0090-6964. http://link.springer.com/10.1007/s10439-013-0833-3 (2013).
4. Clark, A. P. *et al.* Leak current, even with gigaohm seals, can cause misinterpretation of stem cell-derived cardiomyocyte action potential recordings. *Europace : European pacing, arrhythmias, and cardiac electrophysiology : journal of the working groups on cardiac pacing, arrhythmias, and cardiac cellular electrophysiology of the European Society of Cardiology.* ISSN: 1532-2092. http://www.ncbi.nlm.nih.gov/pubmed/37552789 (Aug. 2023).
5. Lei, C. L. *et al.* Accounting for variability in ion current recordings using a mathematical model of artefacts in voltage-clamp experiments. *Philosophical transactions. Series A, Mathematical, physical, and engineering sciences* **378,** 20190348. ISSN: 14712962 (2020).
6. Lei, C. L. *Model-Driven Design and Uncertainty Quantification for Cardiac Electrophysiology Experiments* PhD thesis (University of Oxford, 2020).
7. Clerx, M., Collins, P., de Lange, E. & Volders, P. G. A. Myokit: A simple interface to cardiac cellular electrophysiology. *Progress in biophysics and molecular biology* **120,** 100–14. ISSN: 1873-1732. http://www.ncbi.nlm.nih.gov/pubmed/26721671 (Jan. 2016).
8. Virtanen, P. *et al.* {SciPy} 1.0: Fundamental Algorithms for Scientific Computing in Python. *Nature Methods* **17,** 261–272 (2020).